Supplementary information for:

Protein engineering reveals mechanisms of functional amyloid formation in *Pseudomonas aeruginosa* biofilms

Alissa Bleem, Gunna Christiansen, Daniel J. Madsen, Hans Maric, Kristian Strømgaard, James D. Bryers, Valerie Daggett, Rikke L. Meyer, and Daniel E. Otzen

SI Methods

Peptide microarray methods to supplement the protocol found in the main text:

For evaluation in microarray format, peptides were synthesized in parallel using a ResPep SL synthesis robot (Intavis AG, Cologne, Germany) equipped with a Celluspot synthesis module and printed using a slide spotting robot (Intavis AG). Coupling reagents were freshly prepared every 48 h. Synthesis was based on Standard Fluorenylmethoxycarbonyl (Fmoc) peptide synthesis using reagents from Sigma-Aldrich (St. Louis, MO) and Iris (Marktredwitz, Germany) and performed on acid-soluble Fmoc-β-Alanine etherified cellulose disks (area 0.12 cm^2, loading 1.0 µmol cm^{-2}). N-terminal Fmoc protection was removed by adding 2 µL and 4 µL 20% Piperidine in N-Methyl Pyrrolidone (NMP) for 5 and 10 min. Two couplings (each 40 min) using Oxyma/N,N′-Diisopropylcarbodiimide/Amino Acid in the relation (1.1/1.5/1.0) in at least 5-fold excess followed by two washing steps (100 µL and 300 µL NMP) and 4 µL capping solution (5% Acetic Anhydride in NMP) achieved peptide elongation by one amino acid. The subsequent peptide work-up was performed manually on all peptides in parallel after transfer of the cellulose disks into 96 deep-well blocks. Peptide side-chain deprotection was achieved with 150 µL deprotection solution (trifluoroacetic acid (TFA)/triisopropylsilane (TIPS)/water/DCM: 80%, 3%, 5%, 12%) for 2 h. Disks were then solubilized overnight in 250 µL of cellulose solvation solution (TFA/trifluoromethansulfonic acid/TIPS/water: 88.5%, 4%, 2.5%, 5%) under strong agitation. 750 µL diethyl ether (DE, -20°C) was added to the dissolved cellulose−peptide conjugates and the mixture was briefly agitated and kept at -20°C for 1 h. Precipitated conjugates were pelleted by centrifugation at 2000 xg for 30 min at 4°C. After removal of the supernatant the pellet was additionally washed twice with 750 µL fresh DE (-20°C). After the final washing step, residual ether was evaporated and 250 µL of dimethyl sulfoxide (DMSO) was added to re-solvate the cellulose-peptide conjugates. The cellulose-peptide conjugate stock solutions were stored at -20°C. Prior to printing 80 µL of the stocks were transferred to a 384-well plate and mixed with 20 µL SSC buffer (150 µM NaCl; 15 µM $Na_3C_6H_5O_7$; pH 7.0). 50 nL of each peptide was contact printed on coated glass slides with a slide spotting robot (Intavis AG) and dried overnight.

SI Table 1. Sequence analysis of GVNXAA hexapeptides in R1, R2, and R3.

Strain	NCBI Reference	R1 motif	%ID to PAO1 (GVNVAA)	R2 motif	%ID to PAO1 (GVNVAA)	R3 motif	%ID to PAO1 (GVNIAA)
Pseudomonas aeruginosa PAO1	NP_250644.1	GVNVAA		GVNVAA		GVNIAA	
Pseudomonas putida GB-1	WP_012272553.1	GINVAA	83.33	GINIAG	50	GVNVAA	83.33
Pseudomonas putida F1	WP_012052566.1	GINVAA	83.33	GINVAG	66.67	GVNVAA	83.33
Pseudomonas putida BIRD-1	WP_014591276.1	GINVAA	83.33	GINVAG	66.67	GVNVAA	83.33
Pseudomonas putida KT2440	NP_745000.1	GINVAA	83.33	GINVAG	66.67	GVNVAA	83.33
Pseudomonas entomophila L48	WP_011534103.1	GVNVAA	100	GINIAG	50	GVNVAA	83.33
Pseudomonas putida W619	WP_012314614.1	GVNVAA	100	GINVAG	66.67	GVNVAA	83.33
Pseudomonas sp. UK4	EEP64551.1	GANIAA	66.67	GVNVAA	100	GVNVAA	83.33
Pseudomonas fluorescens A506	WP_003190893.1	GVNAQS	50	GYNGQA	50	GVNLQS	50
Pseudomonas fluorescens SBW25	WP_012723889.1	GVNVQA	83.33	GYNGQA	50	GVNLQS	50
Pseudomonas fluorescens WH6	ZP_07775110.1	GVNVQA	83.33	GYNGQA	50	GVNLQS	50
Pseudomonas synxantha BG33R	ZP_10141134.1	GVNVQS	66.67	GYNGQS	33.33	GVNLQS	50
Pseudomonas sp. S9	ZP_09711309.1	GINVVA	66.67	GANVAA	83.33	GVNVAA	83.33
Pseudomonas aeruginosa 2192	ZP_04933660.1	GVNVAA	100	GVNVAA	100	GVNIAA	100
Pseudomonas aeruginosa C3719	ZP_04928363.1	GVNVAA	100	GVNVAA	100	GVNIAA	100
Pseudomonas aeruginosa LESB58	WP_003113480.1	GVNVAA	100	GVNVAA	100	GVNIAA	100
Pseudomonas aeruginosa PACS2	ZP_01365301.1	GVNVAA	100	GVNVAA	100	GVNIAA	100
Pseudomonas putida S16	WP_013972458.1	GVNVAA	100	GINIAG	50	GVNVAA	83.33
Pseudomonas aeruginosa 39016	ZP_07797129.1	GVNVAA	100	GVNVAA	100	GVNIAA	100
Pseudomonas aeruginosa DK2	WP_003088317.1	GVNVAA	100	GVNVAA	100	GVNIAA	100
Pseudomonas aeruginosa NCGM2.S1	WP_003088317.1	GVNVAA	100	GVNVAA	100	GVNIAA	100
Pseudomonas aeruginosa PAb1	ZP_06879114.1	GVNVAA	100	GVNVAA	100	GVNIAA	100
Pseudomonas aeruginosa UCBPP-PA14	WP_003088317.1	GVNVAA	100	GVNVAA	100	GVNIAA	100
Pseudomonas sp. 2_1_26	ZP_09055487.1	GVNVAA	100	GVNVAA	100	GVNIAA	100
Pseudomonas aeruginosa M18	WP_003121980.1	GVNVAA	100	GVNVAA	100	GVNIAA	100
Pseudomonas sp. M47T1	ZP_10148953.1	GVNVAG	83.33	GINVTS	50	GANVAS	50
Pseudomonas fluorescens Pf0-1	WP_011334011.1	GMNNTA	50	GVNNSA	66.67	GYNNAA	66.67
Pseudomonas brassicacearum NFM421	WP_003202372.1	GANIAA	66.67	GINVTA	66.67	GANVSA	50
Pseudomonas fluorescens F113	WP_014338150.1	GANIAA	66.67	GINVTA	66.67	GANVSA	50
Pseudomonas chlororaphis O6	ZP_10175099.1	GANVAA	83.33	GINVTA	66.67	GANVSA	50
Pseudomonas protegens Pf-5	WP_011061407.1	GANVAA	83.33	GINVTA	66.67	GANVSA	50
AVERAGE %ID to PAO1			**85.5**		**75.6**		**78.9**

SI Table 2. Bacterial strains and primers used in this study.

Name	Description	Reference
P. aeruginosa PAO1 WT	Wild-type; no mutation	-
P. aeruginosa PAO1 pFap	PAO1 with pMMB90Tc-PAO1fap plasmid encoding *fapA-fapF*, Tet resistant	Dueholm et al. (2013)
pET30a(+) FapC C304S/C307G: forward primer	CCGGGCCGCTGCTGCTACC	This study
pET30a(+) FapC C304S/C307G: reverse primer	CGGGTGGTGAAAGCCTGG	This study

SI Table 3. ZipperDB analysis of FapC mutants in R1, R2, R3, NC, and PC. RE = Rosetta energy. Values in *italics* indicate no change from wild-type; values in **bold** indicate change from wild-type; mutation sites (GVNXAA → KFDDTK) are underlined in the sequences below.

	Average RE, full sequence (kcal/mol)	Average RE in R1 (kcal/mol)	Average RE in R2 (kcal/mol)	Average RE in R3 (kcal/mol)	Change from WT, full sequence (kcal/mol)	Change from WT, within repeat (kcal/mol)
FapC WT	*-21.84*	*-21.96*	*-21.59*	*-22.93*	–	–
FapC R1	**-21.72**	**-21.23**	*-21.59*	*-22.93*	**+0.12**	**+0.73**
FapC R2	**-21.71**	*-21.96*	**-20.65**	*-22.93*	**+0.13**	**+0.94**
FapC R3	**-21.69**	*-21.96*	*-21.59*	**-21.58**	**+0.14**	**+1.35**
FapC NC	**-21.79**	*-21.96*	*-21.59*	*-22.93*	**+0.05**	–
FapC PC	**-21.84**	*-21.96*	**-21.82**	*-22.93*	**-0.004**	**-0.23**
FapC TM	**-21.44**	**-21.23**	**-20.65**	**-21.58**	**+0.40**	–

Wild-type R1 sequence:
QQNYNNKVSNFGTLNNASVSGSIKDASGNVGVNVAAGDNNQQANAAALA
Wild-type R2 sequence:
QSGYGNTLNNYSNPNTASLSNSANNVSGNLGVNVAAGNFNQQKNDLAAA
Wild-type R3 sequence:
NNASLSNSLQNVSGNVGVNIAAGGGNQQSNSLSI

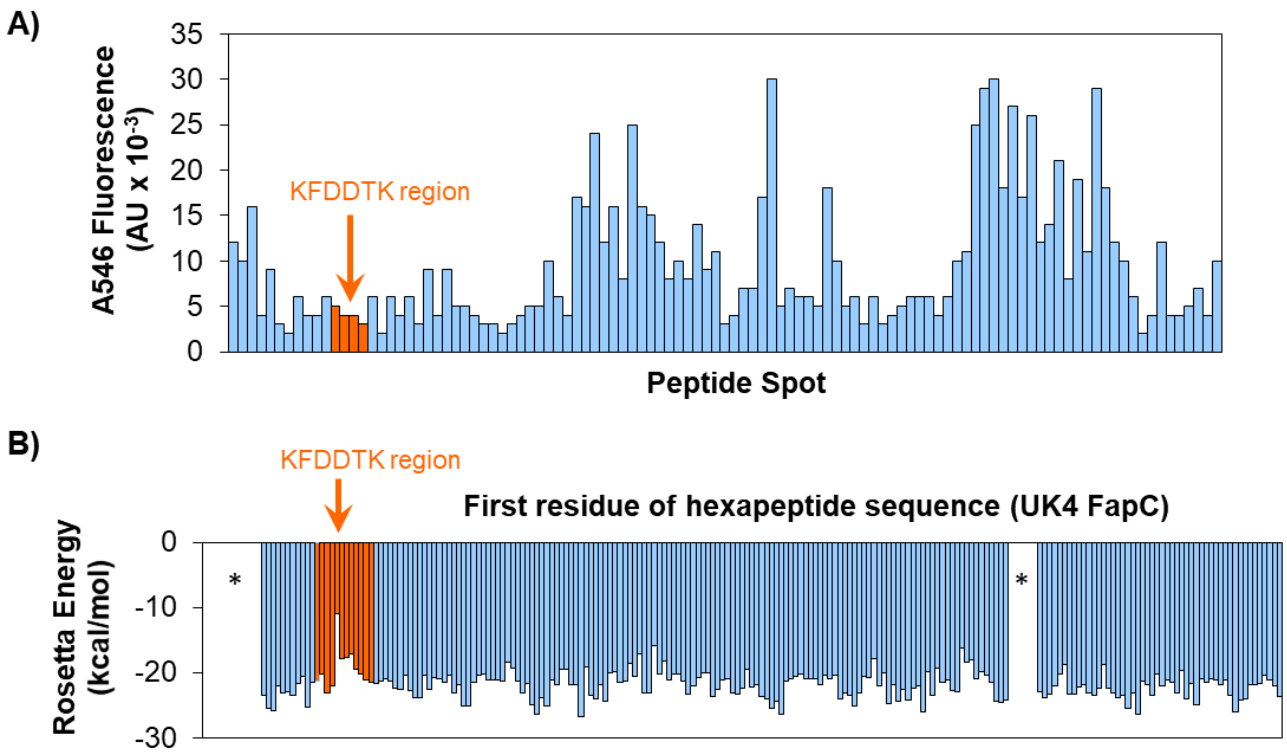

SI Figure 1. A) Relative fluorescence intensity of A546-labeled UK4 FapC on cellulose peptide array, plotted against each spot peptide sequence of UK4 FapC. Bars highlighted in orange indicate peptide spots containing the KFDDTK sequence. **B)** Rosetta energies for each hexapeptide segment of the UK4 FapC sequence. Candidate sequences were taken from the area shaded in orange, and the sequence KFDDTK was ultimately selected for PAO1 FapC mutations due to its combination of relatively high Rosetta energy (low amyloid propensity) and net neutral charge. *Proline residues are incompatible with the 3D profile method in ZipperDB; hexapeptides with prolines are therefore unscored.

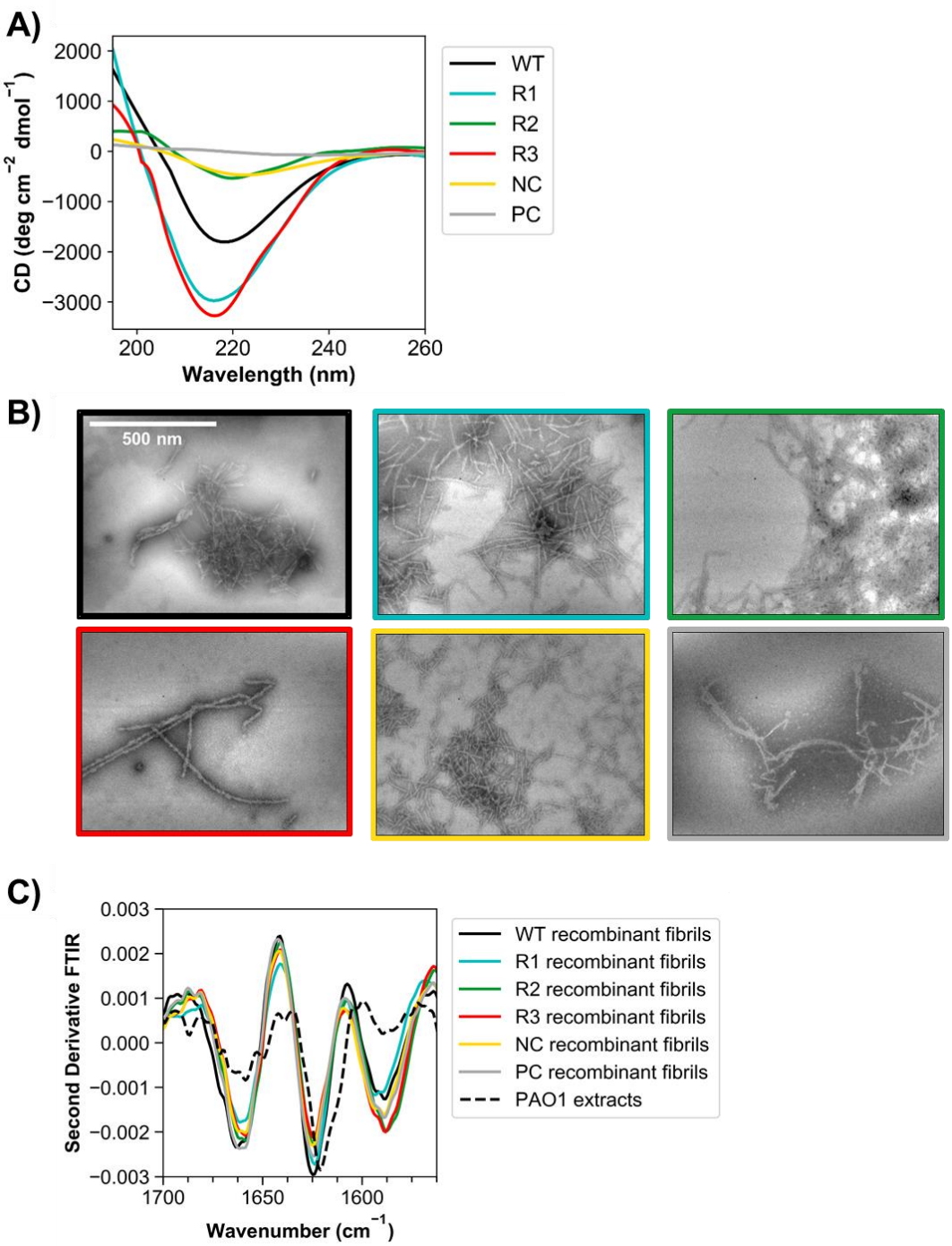

SI Figure 2. A) Conversion to β-sheet secondary structure was verified by CD for FapC WT and five mutants. The positive control, PC, has a null signal because the sample consisted almost entirely of insoluble fibrils. **B)** The presence of amyloid fibrils was also confirmed by TEM. Border colors match the legend in "A" and scale in upper left image applies to all images. **C)** FTIR comparison of recombinant FapC fibrils (solid lines) compared to Fap fibril extract (dashed line) from *P. aeruginosa* PAO1 pFap (**SI Table 2**). Second derivative minima at ~1625 cm^{-1} indicate β-sheet structure.

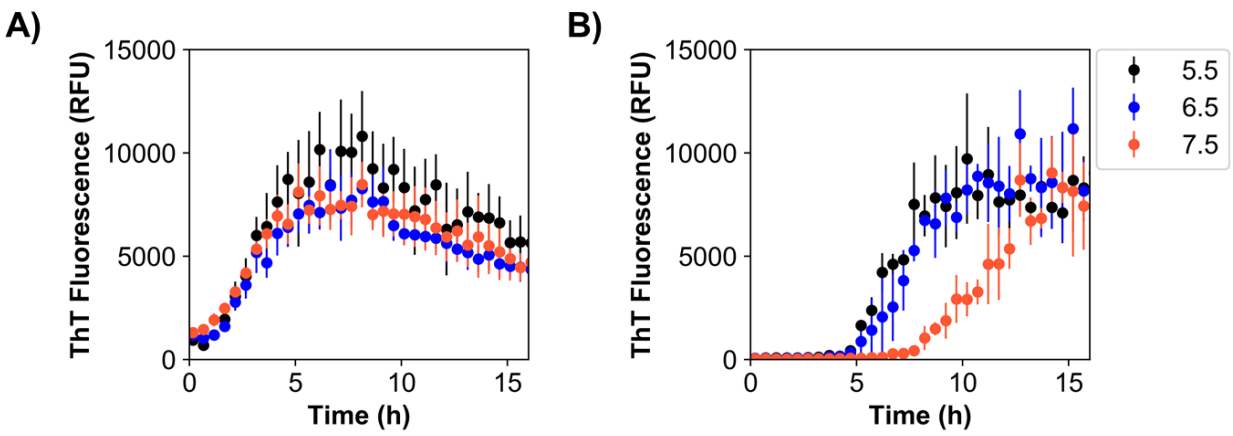

SI Figure 3. A) FapC WT and **B)** FapC R3 mutant were incubated with shaking at 37°C in 10 mM Tris buffer, pH 5.5 (black), 6.5 (blue), and 7.5 (orange). ThT fluorescence indicates amyloid fibril formation, and error bars represent the standard deviation from the mean of three replicates.

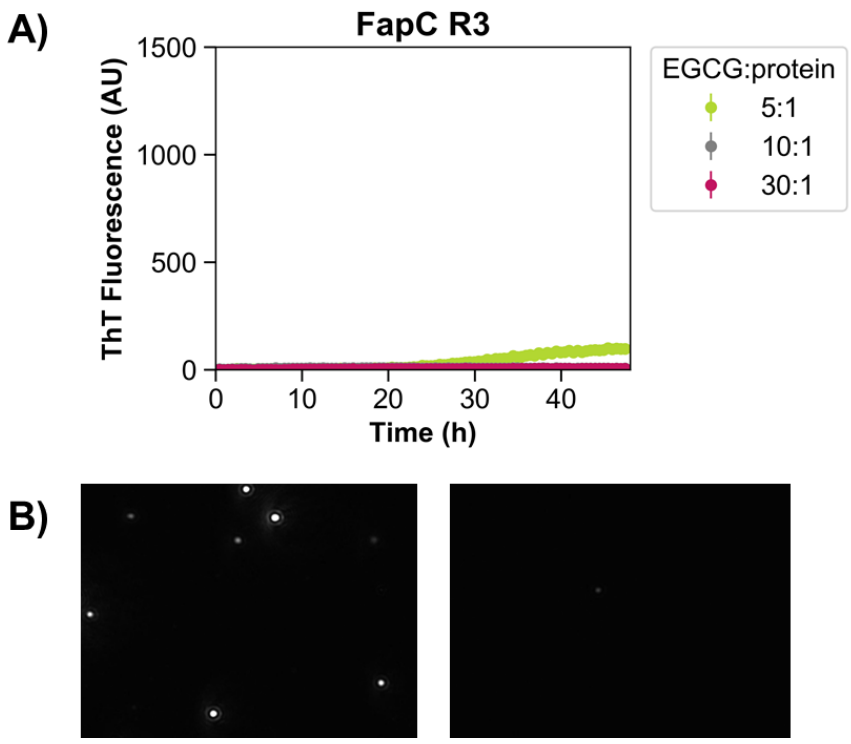

SI Figure 4. A) ThT fluorescence never increased above baseline for FapC R3 samples incubated with 10:1 or 30:1 molar ratio of EGCG:protein. A faint, but significant, increase in fluorescence after ~30 h indicated some weak fibrillation at a 5:1 molar ratio. **B)** NTA analysis of (*left*) 90 μM EGCG solutions indicate some small colloidal particles when compared to (*right*) buffer alone. EGCG remains polydisperse and does not appear to form colloidal particles at lower concentrations.

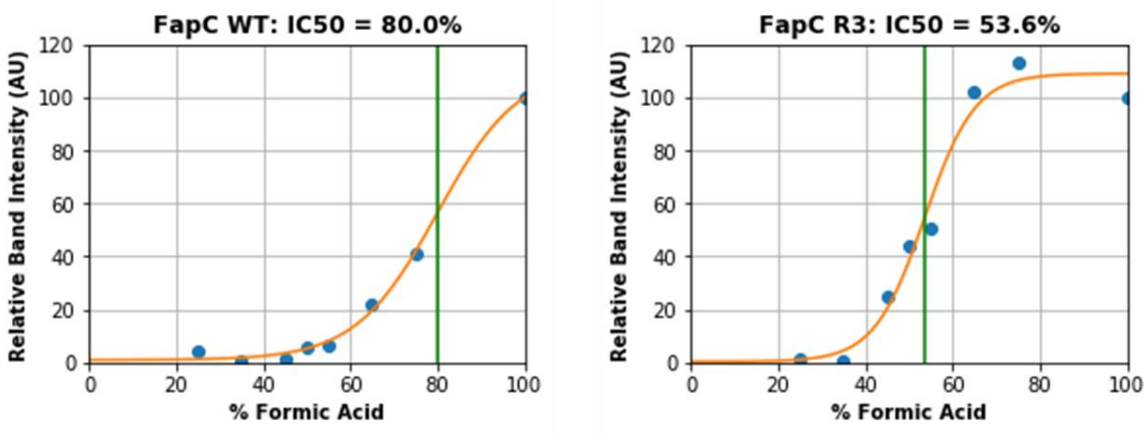

SI Figure 5. FA dissolution data (blue circles) from Figure 5B were regressed using least-squares regression and a sigmoidal fit (orange lines) of the form in equation (1) below. The parameter x_0 defines an "IC50", i.e. the concentration of FA at which relative band intensity reaches half-maximum (green vertical lines).

$$y = \frac{c}{1+e^{-k(x-x_0)}} + y_0 \qquad \text{(Eq. 1)}$$

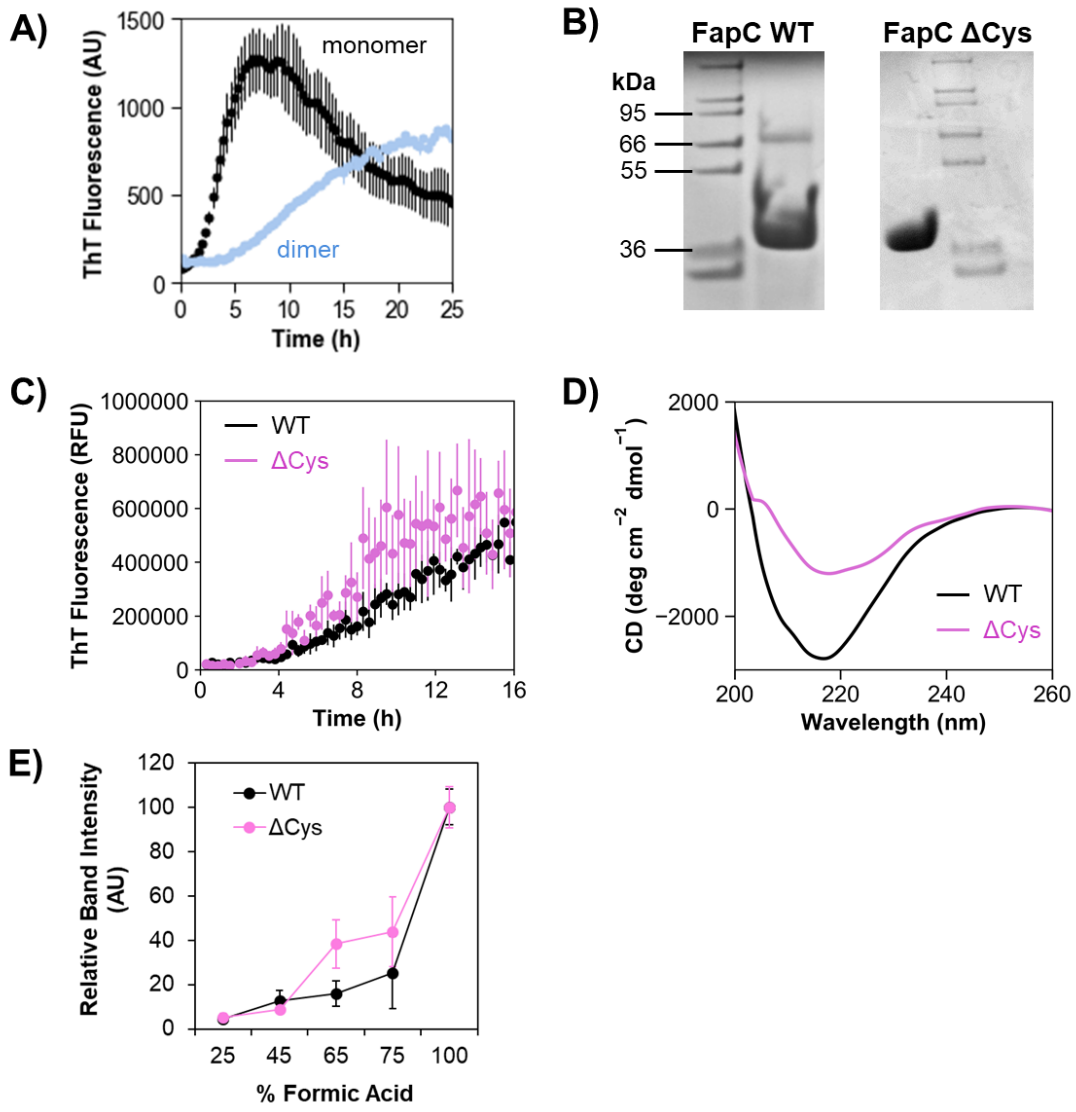

SI Figure 6. A) Isolated fractions of the FapC WT dimer species were pooled and concentrated to 0.5 mg/mL, and then aggregation of the dimer was tracked using ThT fluorescence. Dimer (0.5 mg/mL) is shown in blue and monomer (0.2 mg/mL) is shown for comparison in black. **B)** SDS-PAGE of purified FapC WT and ΔCys demonstrates the lack of disulfide-mediated dimers in ΔCys. Note that FapC runs slightly higher than its molecular weight of ~32 kDa; this is typical behavior for this protein on polyacrylamide gels. **C)** ThT assay to compare fibrillation profiles of FapC WT (black) and FapC ΔCys (pink). Error bars in (A) and (B) indicate standard deviation from the mean of three replicates. **D)** CD spectra for endpoint samples of FapC WT (black) and FapC ΔCys (pink) indicate conversion to β-sheet secondary structure. **E)** Formic acid treatment of WT fibrils (black) versus ΔCys fibrils (pink) demonstrates that disulfide bonding capability leads to a moderate increase in fibril stability.

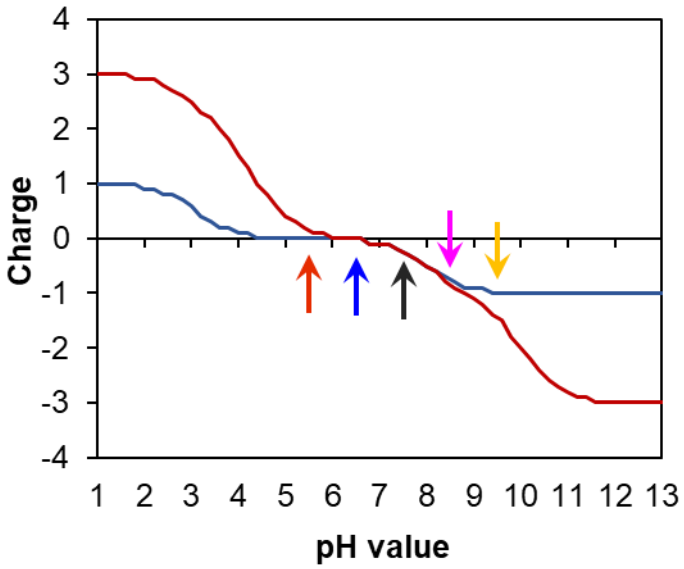

SI Figure 7. pH versus predicted charge state within the R3 repeat segment (residues 267-300) of FapC. Blue line = wild-type R3 sequence; red line = GVNIAA→KFDDTK mutated R3 sequence. Arrow colors correspond to pH values tested in Figure 3: red = pH 5.5, blue = pH 6.5, black = pH 7.5, pink = pH 8.5, and yellow = pH 9.5. Charges were predicted using the ThermoFisher Peptide Analyzing Tool.